The observational response of MAXI onboard ISS.

Naoki Isobe[a], Masaru Matsuoka[a], Shiro Ueno[a], Hiroshi Tomida[a], Kazuyoshi Kawasaki[a], Haruyoshi Katayama[a], Tatehiro Mihara[ba], Mitsuhiro Kohama[b], Ikuya Sakurai[b], Motoki Nakajima[b], Nobuyuki Kawai[ca], Jun Kataoka[ca], Atsumasa Yoshida[da], Daiki Takahashi[d], Masami Uzawa[d], Hiroshi Tsunemi[ea], Emi Miyata[ea], and Isao Tanaka[f]

[a] National Space Development Agency of Japan (NASDA), Tsukuba Space Center
[b] Cosmic Radiation Laboratory, Institute of Physical and Chemical Research (RIKEN)
[c] Department of Physics, Tokyo Institute of Technology
[d] Department of physics, Collage of Science and Engineering, Aoyama Gakuin University
[e] Department of Earth and Space Science, Osaka University
[f] Meisei Electric Co., Ltd.

ABSTRACT

The current status is reported of the development of Monitor of All-sky X-ray Image and the measurement of its observational response. MAXI is a scanning X-ray camera to be attached to the Japanese Experiment Module of the International Space Station in 2008. MAXI is mainly composed of two kinds of instruments, GSC which is sensitive to the 2 – 30 keV photons, and SSC to the 0.5 – 10 keV ones. As an X-ray all-sky monitor, MAXI has an unprecedented sensitivity of 7 mCrab in one orbit scan, and 1 mCrab in one week.

Using the engineering mode of the proportional counter and of the collimator for GSC, the observational response of GSC is extensively measured. The acceptable performances are obtained as a whole for both the collimator and the counter. The engineering models of the other part of MAXI are also constructed and the measurement of their performance is ongoing.

Keywords: MAXI, International Space Station, X-Ray, all sky monitor, GSC, SSC, observational response.

1. INTRODUCTION TO MAXI

Monitor of All-sky X-ray Image (MAXI)[1,2,3] is an astronomical payload to be mounted on the Japanese Experiment Module (JEM) - Exposed Facility (EF) of the International Space Station (ISS). MAXI is now scheduled to be launched by H-II A rocket in 2008, and its mission life is expected to be two years after the launch. The overall configuration and the basic concept of MAXI is shown in Figure 1, and the parameters of these instruments are summarized in Table 1. The science instrument of MAXI is mainly consists of two kinds of scanning X-ray camera with a narrow field of view (FOV), Gas Slit Camera (GSC) and the Solid-state Slit Camera (SSC). Both instruments are combination of a narrow slit, a collimator, and a one dimensional position sensitive detector. As a position sensitive detector, GSC and SSC utilize proportional counter and X-Ray CCD chips, respectively. As schematically drawn in the center panel of Figure 1, both instruments have the forward and the zenith FOV, because there are non-operational period in the orbit such as the South Atlantic Anomaly. Therefore, MAXI can scan through almost the whole sky twice in every 90 minutes, in the course of the orbital motion of the ISS.

One of the most prominent characteristics of MAXI is its high sensitivity, as an all sky X-ray monitor in the 0.5 – 30 keV range. MAXI is expected to detect the X-ray sources with the brightness of 7 mCrab in one orbit scan, and with 1 mCrab in one week. Therefore, MAXI is able to monitor not only the Galactic sources, such as black holes, neutrons stars, X-ray novae and supernovae, but also extra-Galactic sources like active galactic nuclei and clusters of galaxies. Moreover, MAXI will challenge explore the large scale structure of the universe, by probing the distribution of the cosmic X-ray background.

Further author information: (Send correspondence to N.I.)
N.I.: E-mail: isobe@oasis.tksc.nasda.go.jp Telephone: +81 29 868 3781
M.M.: E-mail: matsuoka.masaru@nasda.go.jp Telephone: +81 29 868 3780, Address: National Space Development Agency of Japan (NASDA), Tsukuba Space Center 2-1-1, Sengen, Tsukuba, Ibaraki, 305-8505, Japan

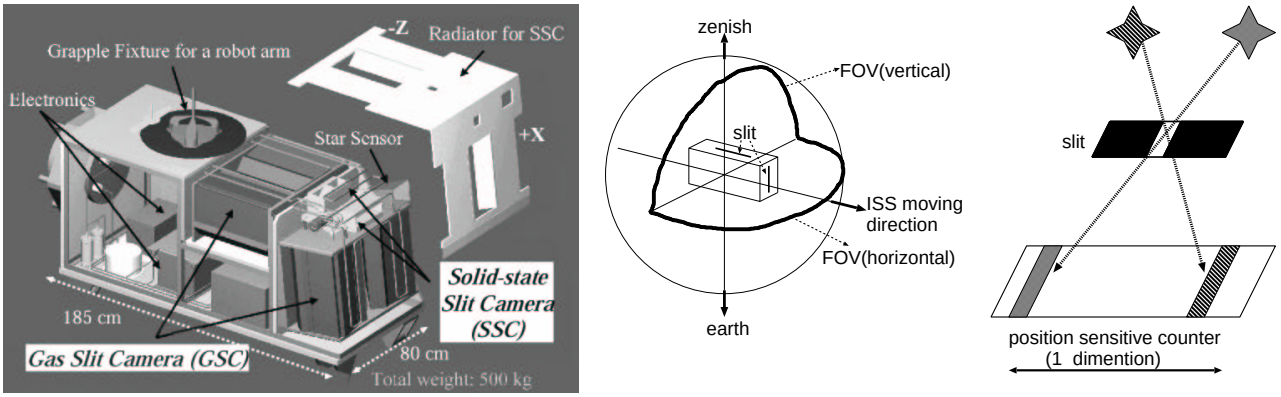

Figure 1. (left) The overall configuration of MAXI. The total weight of MAXI is 500 kg, and its length, width, and height is 185 cm, 80 cm, and 100 cm, respectively. (center) The schematic drawing of the forward and zenith FOVs of MAXI. (right) The schematic drawing which shows how to determine the position of the celestial sources within the FOV.

Table 1. The basic performance of GSC and SC.

	GSC	SSC
Detector	proportional counter	X-ray CCD Camera
	Xe + CO_2 (1 %) gas	
Energy Range	2 – 30 keV	0.5 – 10 keV
Effective Area	5350 cm^2	200 cm^2
Field of View	1.5 × 160 $degree^2$	1.5 × 80 $degree^2$
Energy Resolution	∼ 18%	$\lesssim$ 150 eV @ 5.9 keV
Spatial Resolution	∼ 1 mm	0.025 mm (pixel size)

2. OBSERVATIONAL RESPONSE OF GSC

We have extensively measured the response of GSC, by using the engineering models (EM) of the counter and that of the collimator for GSC. These results are as a whole acceptable, and we here briefly review them.

2.1. Overview of GSC

The right panel of Figure 2 shows the configuration of a unit of GSC. It is consists of a combination of the two one-dimensional position sensitive proportional counters and the slats collimator. There is a narrow slit, on the top of the collimator. In order to cover 1.5 × 160 degree, three units are used for the forward and the zenith FOV, respectively. Thus in total, twelve proportional counters are used in GSC.

The counter of GSC is constructed by Metorex company in Finland. The top view of the counter is shown in the center panel of Figure 2. The X-ray entrance window is made of Be sheet with a thickness of 100 μm. The size of the window is 272 × 190 mm^2, which is similar to the A4 paper, and its opening area is 445 cm^2. The body of the counter is made of Ti, because it has a similar expansion coefficient to Be. In the counter, the mixture of Xe gas and CO_2 gas (1 %) is filled with the total pressure of 1.4 atm at 0 °C. In the right of Figure 2, the cross sectional view of the counter is shown. For the anodes of the X-ray detection part, 6 carbon wires are used (**C0** – **C5** in Figure 2). Their diameter, length, and resistance are 10μm, 333 mm, and 33 kΩ, respectively. They are surrounded by 10 veto cells, in order to reduce background signals.

Typically, the high voltage (HV) of ∼ 1600 V is supplied to each anode. Signals are read out from the both ends of each anodes by charge pre-amplifiers (AMPTEX A225 hybrid IC). In order to obtain the energy of an incident X-ray photon, the signals of the pulse height from the right side of the anode R and that from the left side L are summed up, and the total pulse height, $PH = R + L$, is analyzed. The event position is estimated

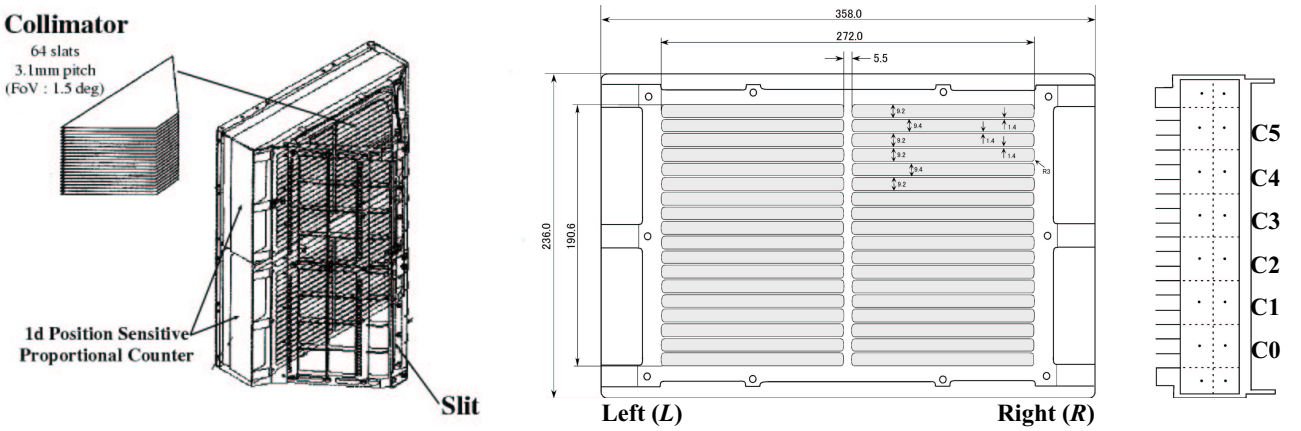

Figure 2. (left) The schematic view of the unit of GSC. (center) The top view of the proportional counter of the GSC. The values in the figure are in written mm. The gray region indicates the Be window through which the incident X-rays are detected. (left) The cross sectional view of the counter.

using the position measure, which is defined as $PM = (R - L)/(R + L)$. Then, if an X-ray photon is absorbed in the right side of the counter. PM becomes positive, and so forth.

The collimator of GSC is mainly composed of 64 slats made of phosphor bronze. The interval between the slats is 3.1 mm and the thickness and the height of each slat is 0.1 mm, 118 cm, respectively. These slats are placed parallel to the anode wire of the counters, and restrict the FOV in the scanning direction to 1.5 degree.

2.2. Energy Calibration

In order to perform the energy calibration of the GSC counter in detail, we have constructed the calibration new equipment which is shown in the right panel of the Figure 3, in the laboratory located in the Tsukuba Space Center of the National Space Development Agency of Japan (NASDA). In order to cover almost all the observable energy range of GSC, 2 – 30 keV, we selected the second targets as summarized in Table 2. Because we plan to perform the low energy calibration for the FM counters with this system, we have carefully selected the targets especially which produces the X-ray lines with energy lower than ~ 4 keV.

We have conducted the energy calibration of the EM counter. Because the gain is reported to be uniform across the all over counter,[4] X-rays from the second targets are pointed at the position 2 cm right from the center of the C0 anode (see Figure 2). Figure 4 shows the PH spectra obtained with the EM counter for the second targets of Mo, Cl, and Ti. The peak of these spectra is usually well reproduced by double Gaussian model, which characterize Kα and Kβ lines of each targets. Based on the fitting using this double Gaussian model, we obtain the relation between the X-ray energy and the PH, as shown in Figure 5. Clearly, the PH is non-linear to the incident energy, and the non-linearity looks more prominent, when the HV value becomes higher. This is because the HV is a little so high in order to improve the position resolution that the counter is

Table 2. A summary of the second targets which are selected for the energy calibration of GSC.

2nd target	Kα (keV)	Kβ (keV)	2nd target	Kα (keV)	Kβ (keV)
S	2.31	2.46	Fe	6.40	7.06
Cl (Vinyl Chloride)	2.62	2.82	Cu	8.05	8.91
Ca (Ca_3N_2)	3.69	4.01	Se	11.22	12.50
Ti	4.51	4.93	Y (Y_2O_3)	14.96	16.74
V	4.95	5.43	Mo	17.47	19.61
Cr	5.41	5.95	Ag	22.16	24.94

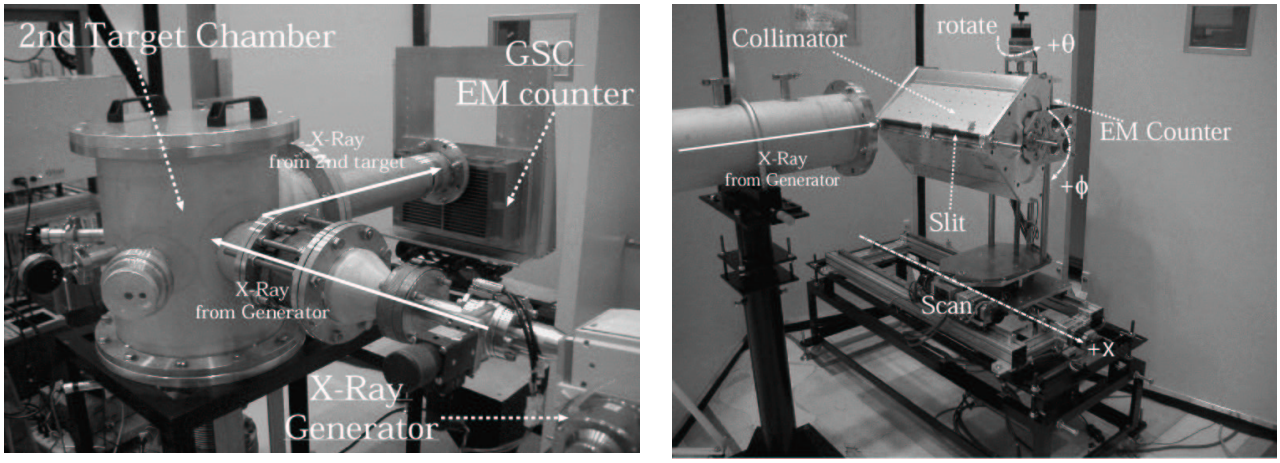

Figure 3. (right) The configuration for the energy calibration of GSC. The first target of the X-ray generator is either Mo, Cu, or Ti. The second fluorescence targets summarized in Table 2 are installed in the chamber. The length, between the second target and the window through which the X-rays come out to the air, is $\sim$ 70 cm. The size of the X-ray window is now 3 mm in diameter. But we plan to make it narrower than $\sim$ 1 mm in the near future, because the position resolution of the counter is near the value. The GSC counter is set up within $\sim$ 1 cm from the X-ray window, for avoiding the soft X-rays ($\lesssim$ 3 keV) to be absorbed by the air. No monochromatic filter is used here, and hence both Kα and Kβ lines of each targets are irradiated to the counter. (left) The configuration in which we have measured the angular response of the GSC collimator. The x, θ and ϕ axes are defined in the figure. The total length of the beam line is 17 m, and then the X-ray beam can be regarded as almost entirely parallel. The diameter of the beam is 0.1 mm.

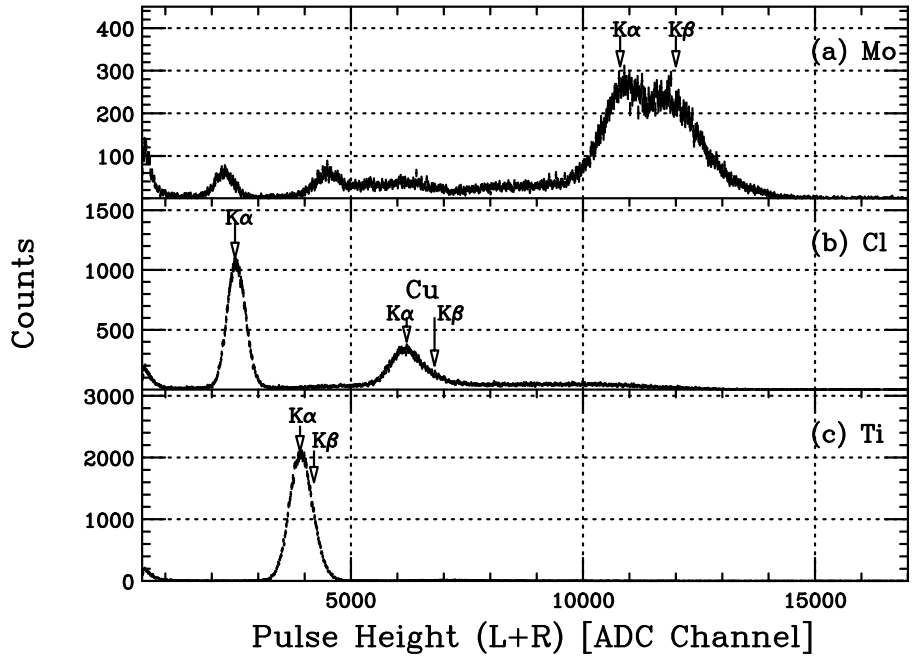

Figure 4. An example of X-ray spectra obtained with the EM1 counter when the second target is (a) Mo, (b) Cl (vinyl chloride), and (c) Ti. The first target of the X-ray generator is Cu. The HV to the anode is set to 1650 V. The X-ray lines from the individual second targets are clearly detected. In the panel (b), the X-ray line of Cu is also detected.

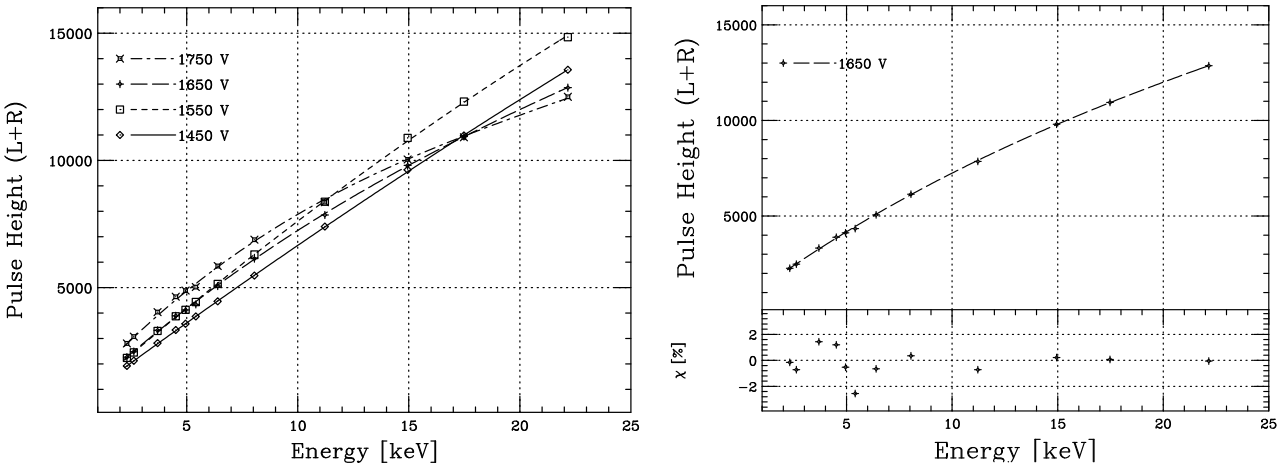

Figure 5. Relations between the incident X-ray energy and the PH obtained with the EM counter. Only the data for Kα lines of individual targets are displayed. The left panel shows the data and the best fit polynomial model, when the HV is 1450, 1550, 1650, 1750 V. The PH is adjusted by the gain amplifier, to be within 2000 – 15000 ADC channel for each HV setup. In the right panel, the data and the best fit third polynomial are shown again, but together with the residuals by the model.

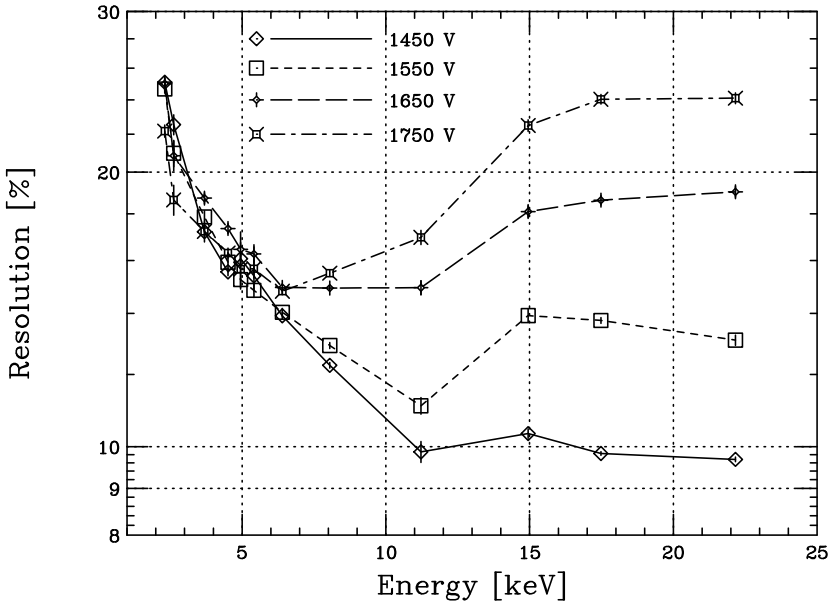

Figure 6. Energy resolution (FWHM) of the EM counter as a function of incident X-ray Energy when the HV is set to 1450, 1550, 1650, 1750 V. Non-linearity of the PH is properly corrected. Only the data for Kα lines of individual targets are displayed.

operated in the limited proportionality region, and that the space charge effect is not negligible. As shown in the right panel of Figure 5, the PH is well described by the second or third polynomials in each HV within the residuals of $\lesssim 2$ %. Around 5 keV, residuals of polynomial fitting become a little large, because of the effect of L absorption edge of Xe gas. We are now extensively measuring and modeling the effect.

Figure 6 shows the energy resolution of the EM counter. Below $\sim$ 7 keV the resolution is nearly inversely proportional to the square root of the incident X-ray energy. But, above $\sim$ 10 keV, the resolution get gradually worse as the energy increases, because of the anomalous gas gain[4,5].

2.3. Position Resolution

As already mentioned in §2.1, we calculate the position of the event on the counter, using the PM value. The left panel of Figure 7 shows the relation between PM and the incident X-ray position. The data is well described by the model curve which is defined as $X = a_0 + a_1 PM - a_2/(PM - a_4) - a_3/(PM - a_5)$, where X is the incident X-ray position, and a_0, a_1, a_2, a_3, a_4, a_5 are free parameters. In the right panel of Figure 7, we show the position resolution. In the typical HV value of $\gtrsim$ 1650 V, the resolution becomes $\lesssim$ 1 mm for Mo Kα lines, and $\lesssim$ 3 mm even for Ti Kα lines.

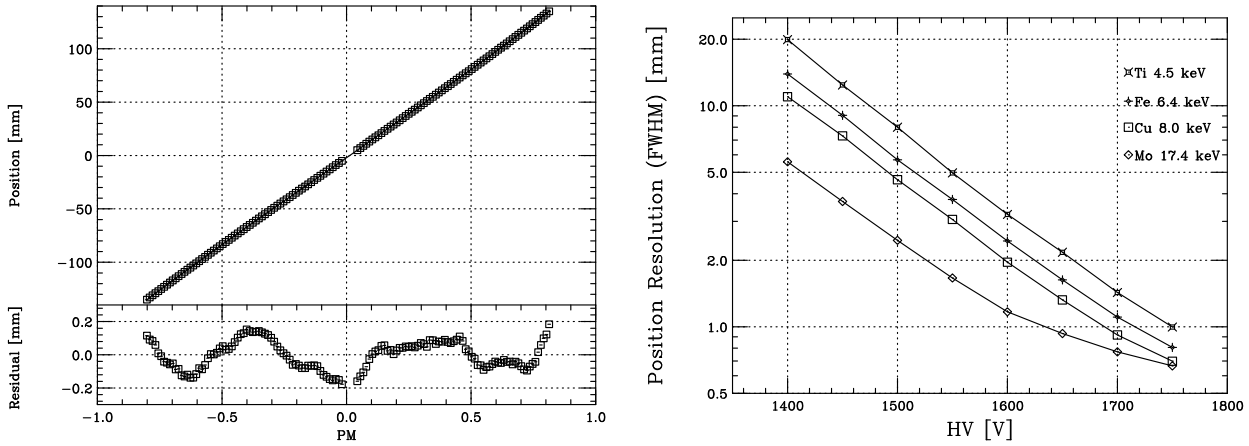

Figure 7. (left) The relation between PM and the position in which the Mo Kα lines are irradiated. The HV value is 1650 V. In the measurement, the size of the X-ray beam is 0.15 mm. (right) The position resolution of the EM counter plotted against the HV value to the anode for Mo, Cu, Fe and Ti Kα lines.

2.4. Uniformity of Efficiency

We next examine the uniformity of the detection efficiency over the EM counter. Because this is especially important in the soft energy band, such as below $\sim$ 3 keV, we have scanned the counter by using the Cl targets. Figure 8 shows the count rate distribution along the C0 anode. The count rate is highly uniform within 1 % for the Cl K lines. This result means that the thickness of Be window is stable within 1.5μm, and that the difference in the detection efficiency is at most 3 % even at 2 keV, the lowest end of the observable range of the GSC.

2.5. Angular Response of Collimator

We have measured the angular response of the GSC collimator in combination with the EM counter, in the setup which is shown in the right panel of Figure 3. We scanned along the slit over the collimator in the x direction by irradiating the X-ray photons from the Mo targets. We changed the value of θ from -1.7 to 1.7 degree. The step of θ is nominally 0.1 degree, and 0.05 degree in $\theta = -0.4$ to 0.4 degree. We made these measurements for $\phi = 5$ and 30 degree. The definitions of x, θ, and ϕ is presented in Figure 3.

Figure 9 shows an example of the count rate distribution along the x axis. We can clearly find the X-ray "shadows" created by the slats of the collimator and those by the support structure of Be window (see Figure 2). Based on these profiles, we calculated the effective area of the collimator, corresponding to each value of ϕ.

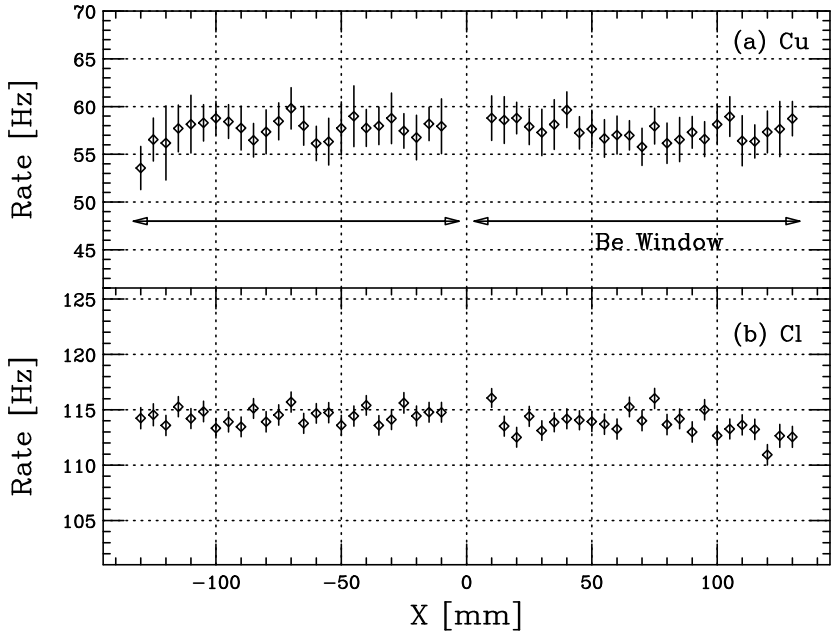

Figure 8. The count rate profile along the C0 anode, obtained in the scanning experiment with the Cl target. The effect of X-ray absorption by the air in front of the counter is properly corrected. The intensity of the X-ray generator is stable well within 1 %. The profile of the Cu lines (see Figure 4) is also shown in the bottom panel (b). The position of the Be window is indicated by the arrows.

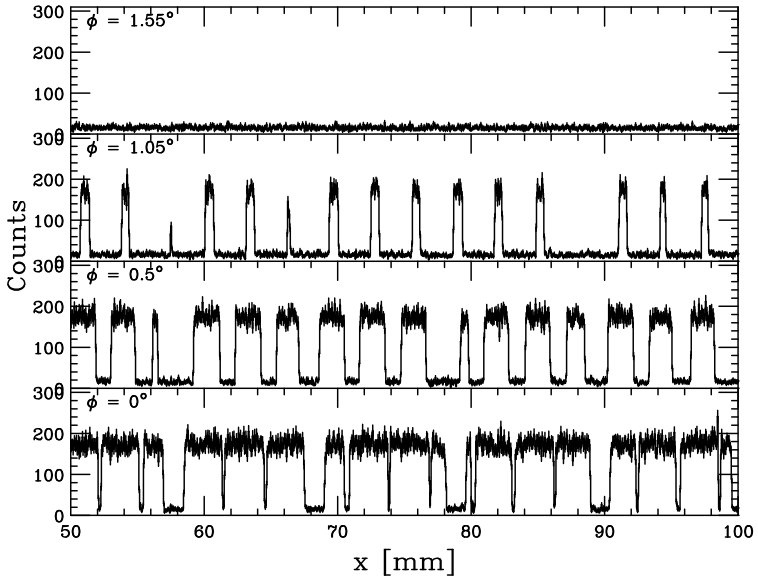

Figure 9. An example of the count rate profile detected by the EM counter through the collimator for $\phi = 1.55$, 1.05, 0.5, and 0 deg. We set $\phi = 5$ degree in the figure. Although only the profile for $x = 50 \sim 100$ mm are shown, the data are taken for $x = 0 \sim 200$ mm, in order to cover the whole collimator. The target of the X-ray generator is Mo. The narrow shadows correspond to the positions of the slats, and the wide ones to the the support structure of the Be windows of the counter.

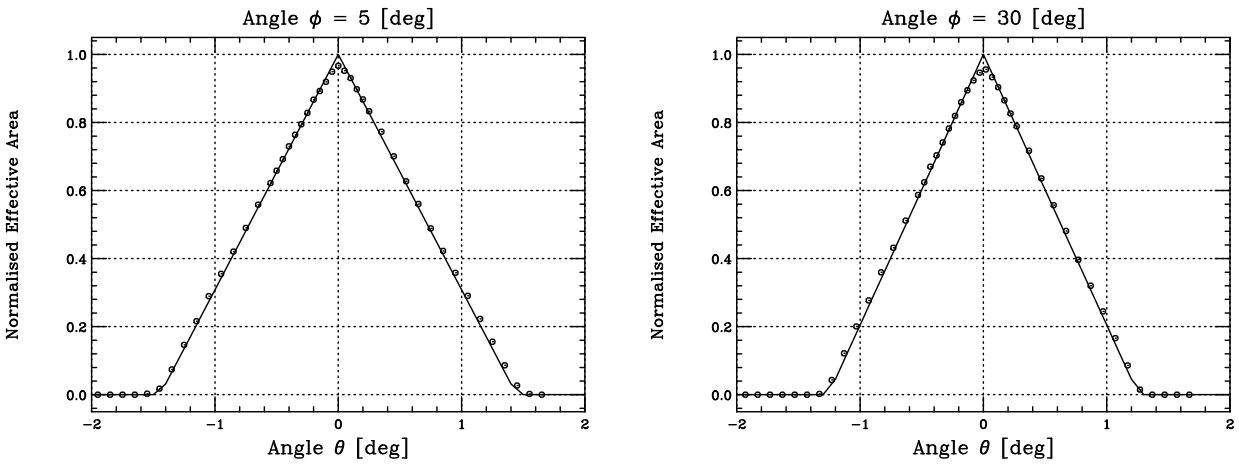

Figure 10. The angular response of the GSC collimator in $\phi = 5$ degree (left) and $\phi = 30$ degree (right). The solid lines in the both panels represent the prediction from the design of the collimator. The θ value is modified in order that the peak of the profile is at $\theta = 0$. The effective area is normalized by the peak value of the model at $\theta = 0$ degree.

We show the angular response of the collimator thus obtained in Figure 10. This profile may include the effect of the position dependency of the detection efficiency of the EM counter. However, the effect is thought to be negligible except for the effect of the Be support structure, because the detection efficiency of the counter is quite uniform as shown in Figure 8. From this experiment, we can find out the following properties of the collimator.

- All the slats are highly parallel within the error of 0.1 degree.
- The pitch of the slats is 3.10 ± 0.07 mm for $\phi = 5$ deg, and 3.12 ± 0.08 mm for $\phi = 30$ deg. These are consistent with the designed value.
- The effective thickness of the slats is is 0.14 ± 0.05 mm for $\phi = 5$ deg, and 0.19 ± 0.07 mm for $\phi = 30$ deg. These are slightly larger than the designed value, but almost acceptable.

Based on these results, the FM collimator will be critically fabricated.

3. OBSERVATIONAL RESPONSE OF SSC

Similar to GSC, the unit of the SSC is mainly a combination of one dimensional position sensitive detector and a slats collimator. As the position sensitive detector, 16 X-Ray CCD chips are used for the SSC unit. The units has a FOV of 1.5×80 degree, and with the two units the forward and the zenith FOVs are covered. The total effective area of SSC with 32 CCD chips become 200 cm^2. The CCD chips are manufactured by Hamamatsu Photonics, and has a size of 1 inch square, which is divided into 1024×1024 pixels with a size of 24 μm. In order to achieve fast readout of many chips, signals are typically binned into 16 pixels in the direction perpendicular to the slats of the collimator, with no need for position resolution. As a result, the total readout time of 16 chips become 10 sec. Figure 11 the spectrum of the ^{55}Fe isotope which is obtained with the EM CCD chip for SSC. An energy resolution of $\lesssim 150$ eV is achieved with the EM chip. The detailed performance of the Flight Model (FM) CCD chips is discussed by Miyata et al. in this conference.[6]

The manufacturing model of the SSC collimator was constructed. The SSC collimator consist of 24 slats which is made of phosphor bronze. The thickness, height, and pitch of slats is 0.1 mm, 91.7 mm, and 2.4 mm, respectively. These restrict the FOV in the scanning direction to 1.5 degree. Each surface of collimator slat is etched to reduce the reflection of soft X-rays. Furthermore, different from the GSC collimator, the slats of the SSC collimator will be plated with chromium (Cr), in order to reduce the reflection of optical light. The angular response of the manufacturing model of the SSC collimator is shown in Figure 12. The data and the model

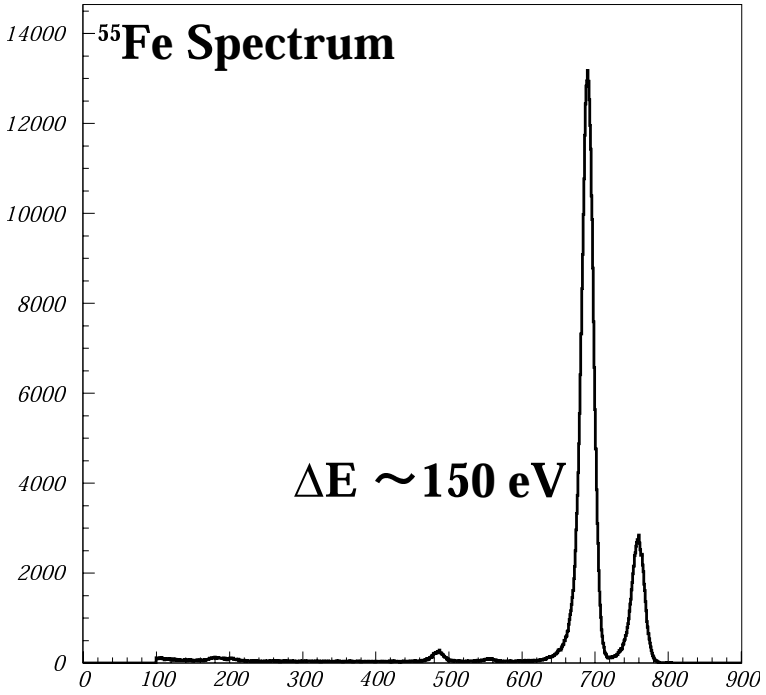

Figure 11. The X-ray spectrum of the ^{55}Fe isotope obtained with the EM CCD chip. Only the events corresponding the the *ASCA* of 0 are selected. The energy resolution of the spectrum is $\lesssim 150$ eV, and Mn Kα and Kβ lines are clearly resolved.

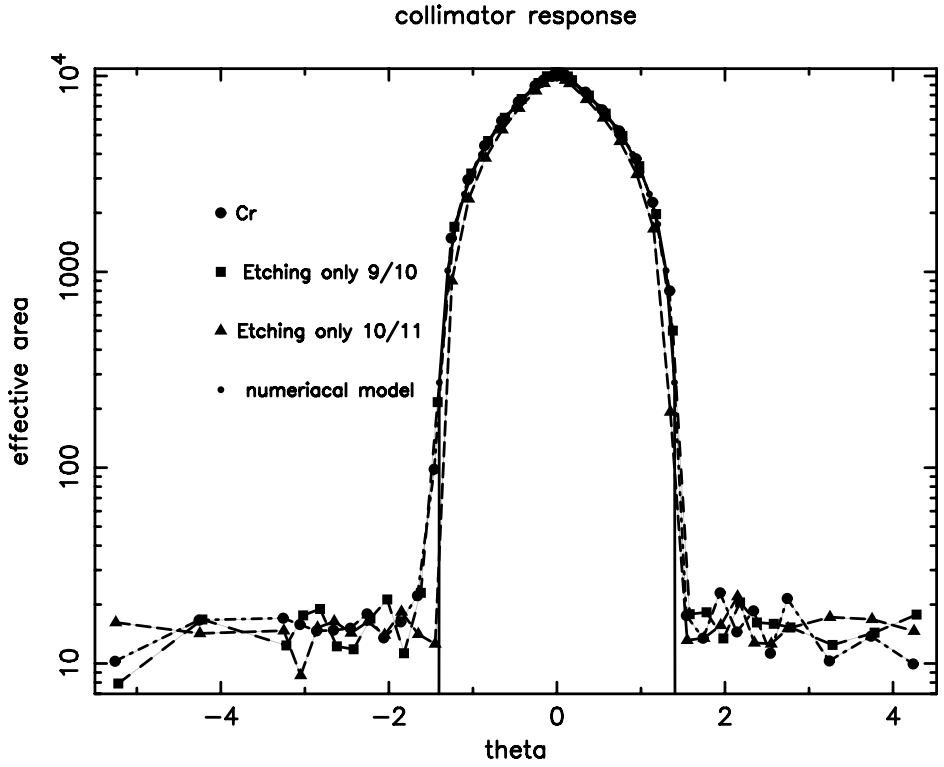

Figure 12. The angular response of the test model of the SSC collimator, with and without Cr plating. The model profile is also shown with the solid line.

profile is almost consistent with each other. The best data are established from the collimator plated with Cr on etching surface. Based on this results, the EM collimator has been built, and the response will be measured in the near future.

4. CURRENT STATUS OF MAXI

Aiming for the launch in 2008, MAXI is now gradually and steadily preparing to manufacture the flight model. For example, the critical design review of all subsystem of MAXI will be completed this year. The Thermal Mechanical Model (TMM) of MAXI was constructed and tested for environments in the launch and in the ISS orbit, last year. The construction of FM of some component, such as the proportional counters of GSC and the CCD chips of SSC have been already started. The selection of the FM CCD chips are reported by Miyata et al. in this conference[6] In the present section, we briefly review some recent topic on the MAXI integration.

4.1. Loop Heat Pipe

The CCD chips of SSC should be cooled down to the operation temperature of -60 °C, in order to reduce dark current and to obtain a sufficient energy resolution. For this purpose, MAXI uses a Loop Heat Pipe (LHP) Radiator System (LHPRS). LHPs differ from conventional heat pipes in that the evaporator only has wick structure inside, and the transport and condenser lines are just smooth small-diameter pipes. The small-diameter pipes with flexible sections save space for routing inside MAXI, and make the payload integration efficient with induced actuation ability of both radiator panels.

The MAXI LHPRS has two condenser lines. The two lines are connected to a single evaporator in parallel. Heat collected at the evaporator from SSC is distributed to the two radiators by two passive flow regulators at the downstream sides of the two radiators; +X radiator with 0.36 m^2 and -Z radiator with 0.53 m^2, where +X and -Z means forward and zenith, respectively (see Figure 1). The regulators work so that the heat flux decreases to a hotter radiator.

We conducted the performance test of the MAXI LHPRS in a vacuum chamber with infrared panels inside simulating sky sinks and with heated frames simulating the MAXI structure. The temperature of the heated frame was set between 0 to 30 °C depending the thermal environment outside MAXI. For three typical combinations of time-averaged sky sink temperatures for two radiators (hot, nominal, and cold cases), we measured equilibrium temperatures of the SSC-evaporator interface at the evaporator side. Inside SSC, Peltier coolers transport heat from CCD chips to the SSC body. In table 3, we show the equilibrium temperatures of the SSC-evaporator interface and the CCD chips. The CCD chips have been actually cooled to the operating temperature.

We have verified that the MAXI LHPRS performs as designed in static sky sink environments. The next step is to verify that, in variable sky sink conditions, the performance meets our requirements.

4.2. Data Processor and Down Link

The X-ray events detected with MAXI are first processed on-board by the Data Processor (DP). The DP has 4 CPUs (R3081, 24MIPS) and 8 MB memory (SRAM) with 1 bit ECC, and they are constructed on the VME bus. The Vx/Works is adopted for the OS, which is capable of handling the internet. The EM of the DP was

Table 3. A summary of test results of LHPRS.

Case	Beta†	SSC-evap. interface	CCD chips
Hot	0°	-9 °C	-58 °C
Nominal	30°	-24 °C	-71 °C
Cold	75°	-32 °C	-79 °C

† The angle between the ISS orbital plane and the line connecting the Earth and the Sun.
The radiator surface is Z93 white paint, and the working fluid is propylene.

developed in June, 2003, and we are measuring the performance of the EM. According to the results from these experiments, we will fix the design of the FM DP by October, 2003.

The DP handles the communication between MAXI and the ground station via JEM/ISS interface. There are two lines for the data down-link, 1553B and Ethernet. The 1553B is low-rate and contains house keeping (HK) and essential data. The ethernet is mid-rate and contains all the information about the detected X-ray. We will use the ethernet data for the detail analysis, but only 1553B data can lead to the minimum success. There are two ways in the down-link to the Tsukuba Space Center, NASDA. One is via the ICS antenna on JEM-EF through Japanese data relay satellites DRTS, and the other is via NASA antenna on ISS, through the USA satellites TDRSS, and NASA center to Tsukuba Space Center. There will be 5 hours of contact at maximum per day in the ICS link when the data can be obtained in real time. The NASA link has 17 hours at maximum. When ISS is out of contact, the data are stored in the ICS data recorder and replayed in the next contact. The real-time contact is essential for making the prompt "alert". The full time coverage is desirable. We are developing the ground analysis softwares for the real-time "alert" system.

4.3. FM Counter for GSC

The vibration test for these counters were performed, as shown in Figure 13. The overall acceleration was provided to the counter during 240 sec, of 14.3 g in root mean square between 20 to 2000 Hz, where g is the acceleration of gravity. This vibration level and duration were determined from the results of the TMM test. After the vibration, we have found no damage on the counter at all. Base on this results, the construction of the FM counters is fully well into the way. At the beginning of July 2003, we have now supplied with five of them. From this summer, we plan to start the ground calibration of the FM counters.

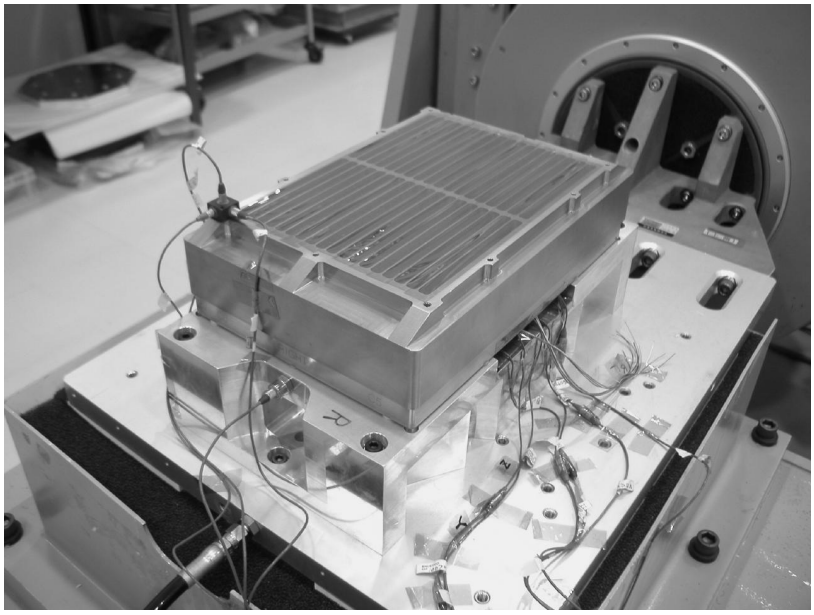

Figure 13. The vibration test for the FM counter of GSC. In front of the counter, polyimide tapes are pasted, in order to protect the Be window (see the next section) from dust and so on. In the picture, vibrations are supplied to the counter in the direction parallel to the anode of the counter (see Figure 2)

5. CONCLUSION

We have confirmed that the EMs of various components of MAXI have as a whole acceptable performances. Now, MAXI is ready to manufacture the FM. From this summer, we will actually start the calibration of the FM of some components.

REFERENCES

1. M., Matsuoka, N., Kawai, T., Mihara, A., Yoshida, H., Kubo, T., Kotani, H., Negoro, B., Rubin, H., Shimizu, H., Tsunemi, K., Hayashida, S., Kitamoto, E., Miyata, M., Yamauchi, "MAXI (monitor of all-sky x-ray image) for JEM on the Space Station" *Proc. SPIE*, **3114**, 414, 1997
2. H., Tomida, M., Matsuoka, S., Ueno, K., Torii, M., Sugizaki, W., Yuan, S. Komatsu, Y., Shirasaki, N., Kawai, A., Yoshida, T., Mihara, I., Sakurai, H., Negoro, H., Tsunemi, E., Miyata, M., Yamauchi, I., Tanaka, "The MAXI mission on the International Space Station" *Proc. SPIE*, **4012**, 178, 2000
3. T.Mihara, M.Matsuoka, S.Ueno, H.Tsunemi, N.Kawai, and the MAXI team "Monitor of All-sky X-ray Image (MAXI) and JEM-EF" *Proc. ISS Utilization conference an AIAA Conference*, **2001-4973**, 387, 2001
4. T., Mihara, N., Kawai, A., Yoshida, I., Sakurai, T., Kamae, M., Matsuoka, Y., Shirasaki, M., Sugizaki., W., Yuan and I., Tanaka, " Performance of the GSC engineering-counter for MAXI/ISS ", *Proc. SPIE*, **4497**, 173, 2001
5. I., Sakurai, T., Mihara, N., Kawai, A., Yoshida, Y., Shirasaki, M., Matuoka, M., Sugizaki, and T., Kamae, "Dependence of gas gain on x-ray-absorbed position in the proportional counter " *Proc. SPIE*, **4140**, 511, 2000
6. E. Miyata, D. Kamiyama, H. Kouno, H. Tsunemi, H. Tomida, and K. Miyaguchi, "Flight CCD selection for the x-ray CCD camera of the MAXI mission onboard the International Space Station" *Proc. SPIE*, this volume